Document downloaded from:

http://hdl.handle.net/10251/98353

This paper must be cited as:

Gómez-Tejedor, JA.; Rodríguez Hernández, JC.; Gómez Ribelles, JL.; Monleón Pradas, M. (2007). Dynamic mechanical relaxation of poly(2-hydroxyethyl acrylate)-silica nanocomposites obtained by the sol-gel method. Journal of Macromolecular Science Part B. 46(1):43-54. doi:10.1080/00222340601036751

The final publication is available at

https://doi.org/10.1080/00222340601036751

Copyright Informa UK (Marcel Dekker)

Additional Information

Dynamic mechanical relaxation of poly(2-hydroxyethyl acrylate)-silica nanocomposites obtained by the sol-gel method

J.A. Gómez-Tejedor[a], J.C. Rodríguez Hernández[a], J.L. Gómez Ribelles[a,b], M. Monleon Pradas[a,b*]

[a] Center for Biomaterials, Universidad Politécnica de Valencia, P.O. Box 22012, E-46071 Valencia, Spain.

[b] Centro de Investigación Príncipe Felipe, Autopista del Saler 16, 46013 Valencia, Spain

*corresponding author. E-mail address: mmonleon@ter.upv.es

Journal of Macromolecular Science, Part B: Physics, 43:43–54, 2004 DOI: 10.1080/00222340409036751

Abstract

A series of poly(hydroxyethyl acrylate)-silica nanocomposites has been polymerized by the simultaneous sol-gel reaction of the organic monomer and the silica precursor tetraethyl orthosilicate (TEOS). Samples with different silica contents were prepared and their mechanical properties have been investigated by dynamic mechanical spectroscopy (DMS). The application of the time-temperature superposition principle to the isothermal DMS results in the main relaxation region permits to successfully construct master curves. The calorimetric properties of these hybrid materials have also been measured in order to compare the results of DMS and DSC. The presence of a polymer phase formed by polymer chains with reduced mobility has been proved by the DMS results. The main relaxation due to the segmental dynamics of these chains takes place at frequencies around seven decades smaller than in the bulk PHEA homopolymer.

keywords: nanocomposites, dynamic mechanical spectroscopy, poly(2-hydroxyethyl acrylate), tetraethyl orthosilicate, sol-gel reaction

1. Introduction

Polymeric hydrogels are finding many applications in science and industry. However, it is known that the mechanical properties in their swollen state generally are poor. Poly(2-hydroxyethyl acrylate) (PHEA) is a well-known hydrogel (1) with the generally good biocompatibility characteristics of the acrylates (2,3). The purpose of this paper is to describe the mechanical behaviour of a type of hybrid materials based on PHEA.

The sol-gel reaction is an easy method, widely used to introduce an inorganic phase inside a matrix (4-8). By means of acid catalyzed hydrolysis and condensation reactions, the silica precursor tetraethyl orthosilicate (TEOS) is able to produce, in the presence of the organic monomer of hydroxyethyl acrylate (HEA), a silica network. The continuity of this network depends mainly on the initial amount of TEOS when other factors are kept constant, like the ratio between water and TEOS and the amount and nature of catalyst used. Such hybrid materials exhibit a nano-scale dispersion of the silica phase, and for this reason they are usually called nanocomposites. The resulting PHEA-silica nanocomposites are transparent, thus indicating that the size of the silica phase aggregates is smaller than 400 nm (9).

Journal of Macromolecular Science, Part B: Physics, 46:43–54, 2007. DOI: 10.1080/00222340601036751

2. Experimental Section

2.1. Materials

The samples were obtained in a sol-gel process (9) varying properly the quantities of reactants to get the desired final silica weight percentage assuming completion of the sol-gel reactions. All chemicals were used as provided by suppliers. The amounts of reagents used are shown in Table 1.

Table 1. Masses used for obtaining the desired silica content.

Reagent	***Reference***	***Nanocomposite samples***		
	Pure PHEA	***PHEA+10% SiO_2***	***PHEA+15% SiO_2***	***PHEA+30% SiO_2***
HEA [g]	10	10	7	5
BPO [g]	0.2	0.2	0.14	0.1
TEOS [g]	-------	3.8519	4.2824	7.4286
H_2O+HCl [a] [g]	-------	0.7037	0.7824	1.3571

[a] HCl water solution prepared adding 10g of distilled water and 0.51g of hydrochloric acid.

Journal of Macromolecular Science, Part B: Physics 46:4, 747-754, 2007. DOI: 10.1080/00222340601036751

2-Hydroxyethyl acrylate (HEA, 96%, Aldrich) was mixed with benzoyl peroxide (BPO, 97%, Fluka) and mechanically stirred for 30 minutes. Tetraethyl orthosilicate (98%, Aldrich) was added to a hydrochloric acid solution (HCl, 37%, Aldrich) and distilled water, and stirred also for 30 minutes. Afterwards both solutions were mixed together and stirred for another 30 minutes. The resulting solution was poured into a mould to obtain samples in the form of sheets approximately 1 mm thick.

Polymerisation was carried out in two steps, first at 60ºC for 21 hours, and then at 90ºC for 18 hours. Finally, samples were rinsed in boiling distilled water for 24 hours in order to remove any unreacted chemicals, and dried in vacuo at 60ºC.

2.2. Atomic Force Microscopy

Atomic force Microscopy (AFM) was performed in a NanoScope III from Digital Instruments operating in the tapping mode in air. Silicon probes from Nanoworld were used with A force constant of 42 N/m and resonance frequency of 320 kHz. The tapping frequency was slightly lower than the resonance one (around 10%), in which the phase signal was set to zero. The ratio between setpoint and drive amplitudes was kept equal

to 0.8, performing a soft tapping of the nanocomposites' surface. Dried samples were fractured in liquid nitrogen and the surface of fracture was scanned with the AFM.

2.3. DSC experiments

Differential scanning calorimetry was performed with a Pyris 1 analyser (Perkin Elmer). A dry nitrogen flow of 20 ml/min was used in order to enhance heat transfer. The temperature of the equipment was calibrated using indium and zinc as references, while indium's enthalpy of fusion was used to calibrate heat flow. The weight of the measured samples ranged between 5 and 10 mg.

Before measurements, samples were kept in vacuo at 70ºC for 24 hours in order to be sure samples were completely dry. A first scan was done from -40 to 250ºC at a heating rate of 10ºC /min in order to erase the thermal history of the samples. Immediately after, a cooling scan from 250 to -40ºC was done at a controlled cooling rate of 40ºC/min. Finally, the ensuing heating scan at 10ºC/min was recorded. The glass transition temperature T_g was calculated as the temperature of the midpoint of the rise of heat capacity in the transition. The breadth of the glass transition (ΔT_g) was characterised by the temperature interval determined by the intersection of the tangent to the thermogram in the inflection point with the glass and liquid lines. The heat capacity jump at the glass transition (Δc_p) was normalized *per* polymer gram, and determined as the difference between the intersections of the extrapolated glass and liquid lines at the inflection point.

Journal of Macromolecular Science, Part B: Physics, 46:43–54, 2007. DOI: 10.1080/00222340601036751

2.4. DMS experiments

The dynamic mechanical experiments were performed in a Seiko DMS210 analyser at isothermal conditions in the stretching mode. Samples with prismatic geometry and dimensions 15×4.5×0.8 mm were used. The experiments were carried out at different

temperatures: from –6ºC to 110ºC for PHEA+30% SiO_2, from –30ºC to 80ºC for PHEA+15% SiO_2, from –12ºC to 70ºC for PHEA+10% SiO_2, every 2ºC, and from –20ºC to 80ºC every 4ºC for pure PHEA. At each temperature, the frequency was scanned from 0.01 to 20 Hz.

Results

3.1. AFM images

Figure 1 shows the topography of the hybrid materials as seen by AFM. Different areas of 2x2 µm were scanned so that reproducible images were obtained. Nanometric features can be observed in both images with different silica contents, such as the occurrence of aggregates of smaller particles of around 40 nm.

Journal of Macromolecular Science, Part B: Physics, 46:43–54, 2007. DOI: 10.1080/00222340601036751

a)

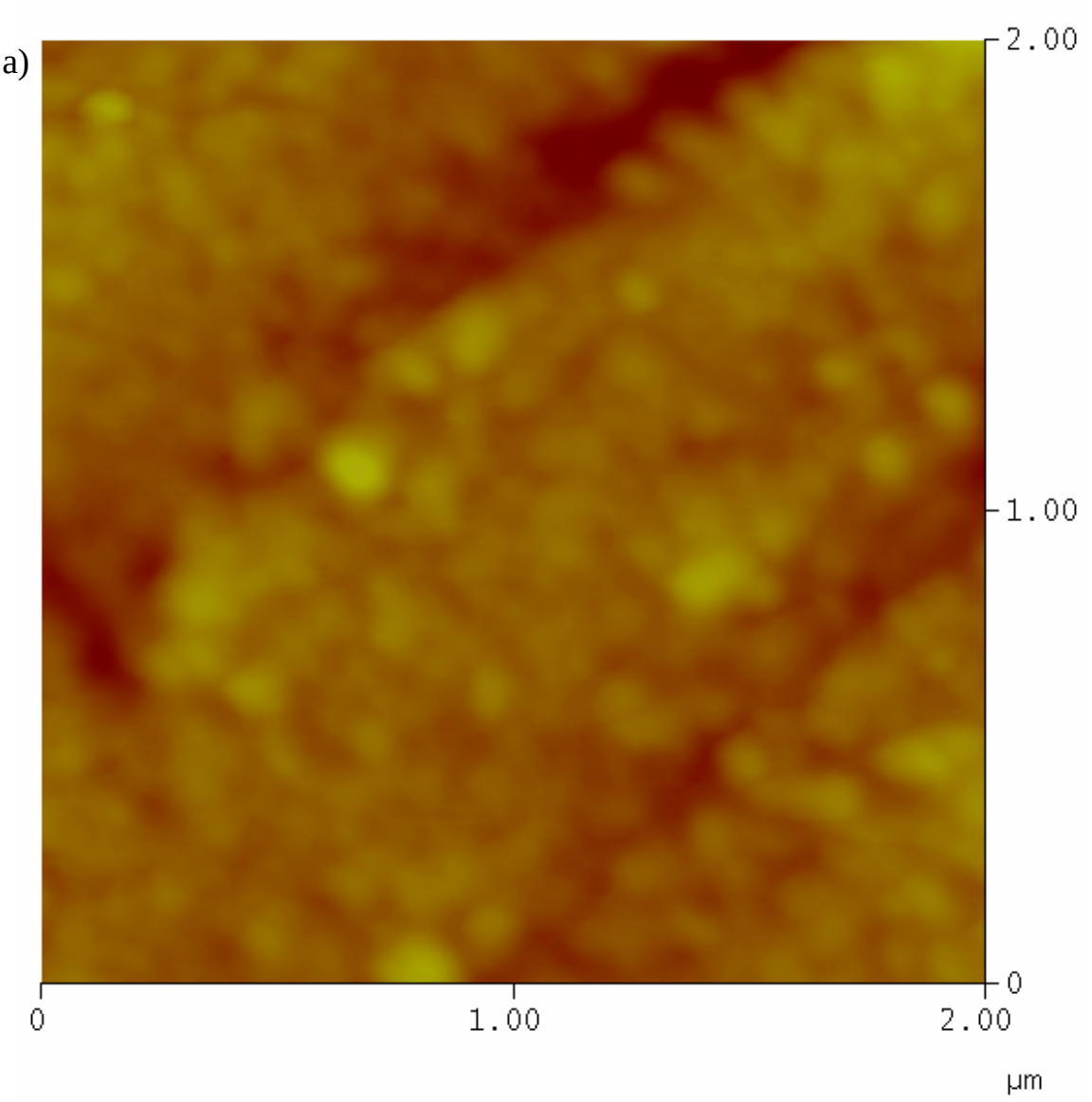

Journal of Macromolecular Sci

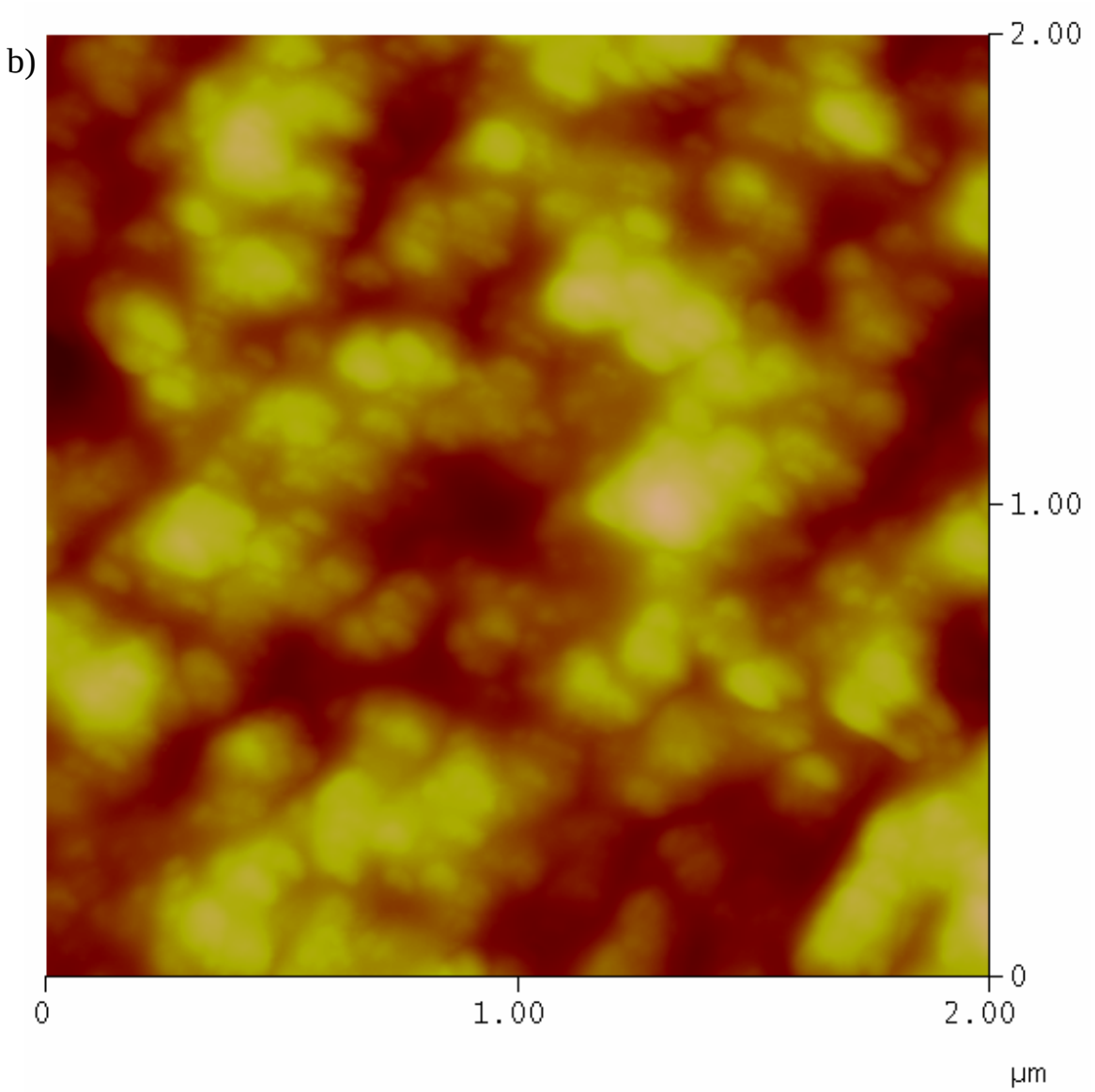

Figure 1. AFM surface topography of hybrid materials: **(a)** PHEA+15% SiO_2 and **(b)** PHEA+30% SiO_2. The colour scale used in both images indicates height range from 0 (dark) to 100 nm (bright).

Journal of Macromolecular Sc.

3.2. DSC results

Figure 2 shows the DSC curves for the second scans (after erasing the previous thermal history) from -30 to 150ºC. There were no substantial differences between the first and the second scan measured. Recorded data above 150ºC are not shown because no other

remarkable phenomenon took place. It has been found out by TGA measurements that degradation starts at temperatures immediately above 250ºC for nanocomposites and pure PHEA (10,11).

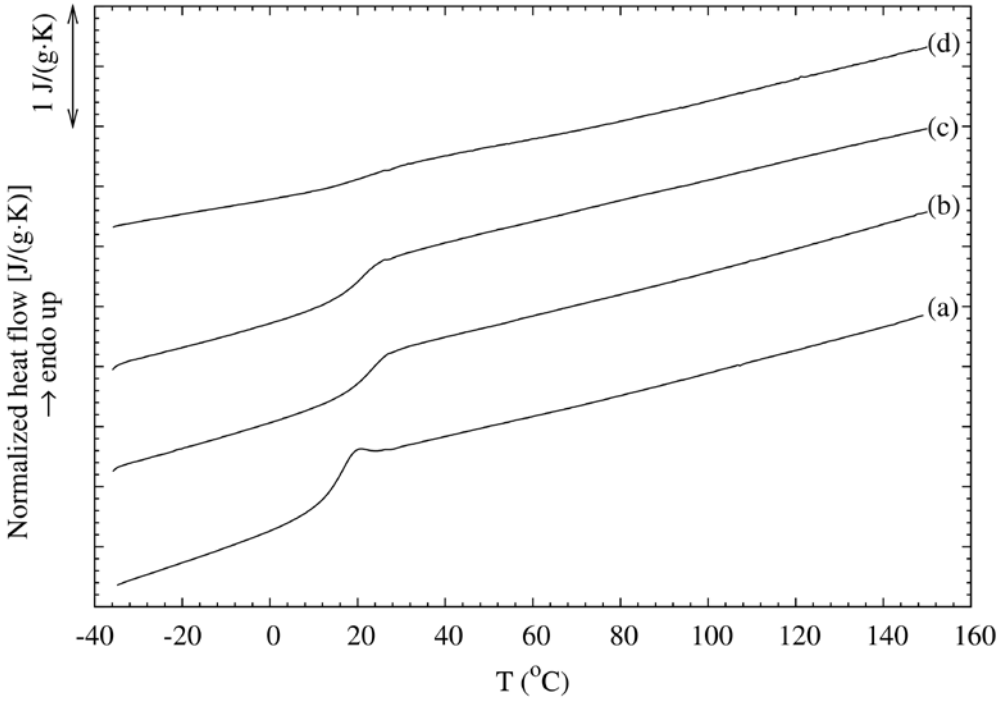

Figure 2. Second DSC scans at a heating rate of 10 K/min: (a) pure PHEA; (b) PHEA+10% SiO_2; (c) PHEA+15% SiO_2; (d) PHEA+30% SiO_2.

Journal of Macromolecular Science

Table 2. Glass transition temperature (T_g) calculated from DSC data, breadth of the glass transition (ΔT_g), specific heat capacity jump at the glass transition (Δc_p), WLF parameters (C_1, C_2), VFTH parameters (T_0, B), coefficient of the volume expansion of the free volume, α_f, and fragility, m, for PHEA with different silica contents. The WLF fit has been done for the shift factors a_T shown in Figure 4, calculated for a reference temperature $T_{ref} = T_g$.

Sample	T_g (K)	ΔT_g(K)	Δc_p (J/gK)	C_1	C_2 (K)	T_0 (K)	B (K)	α_f ($\times 10^3$ K^{-1})	m
Pure PHEA	288.3	8.3	0.40	11.8	55.9	232.5	1514	0.660	60.8
PHEA +10% SiO_2	295.4	12.7	0.32	12.4	89.0	206.5	2539	0.394	41.2
PHEA +15% SiO_2	293.5	13.5	0.31	23.1	145.8	147.6	7745	0.129	46.4
PHEA +30% SiO_2	293.8	20.5	0.10	44.1	253.7	40.1	25774	0.039	51.1

Journal of Macromolecular Science, Part B: Physics, 46:43-54, 2007. DOI: 10.1080/00222340601036751

The glass transition temperatures are shown in Table 2. For the hybrid nanocomposite materials T_g is almost independent of the silica content but higher than that of bulk PHEA. Besides, there is a broadening of the glass transition that can be characterised by its breadth ΔT_g, which is also listed in Table 2. Furthermore it can be observed that the heat capacity jump at the glass transition per polymer gram (Δc_p) decreases as the silica content increases.

The thermograms shown in Figure 2 were recorded after cooling at 40ºC/min from temperatures above the glass transition without any isothermal annealing. The overshoot shown by the thermogram of pure PHEA is due to residual physical aging during the cooling stage; it is characteristic of this kind of thermal history: the height of the peak decreases with increasing cooling rate, and it is smaller in polymers with wide glass transition temperature interval. In the nanocomposites, in which the glass transition broadens, the thermograms do not show this peak although the thermal history of the experiments was the same.

3.3. DMS results

From the isothermal scans the master curves for storage modulus (*E'*) and loss factor (tan δ) were obtained as functions of the reduced frequency $f \cdot a_T$ for a reference temperature T_{ref} = 25^0C (Figure 3). They were constructed by simple shift of the isothermal results along the log *f* axis, according to the time-temperature superposition principle (12). For each sample the shift factors, log a_T, associated with *E'* and tan δ were found to be the same. In principle a small vertical shift due to the temperature dependence of the product $\rho T/\rho T^*$ should also be applied (12), but in this case the correction seemed to be negligible.

2007. DOI: 10.1080/00223460601036351

a)

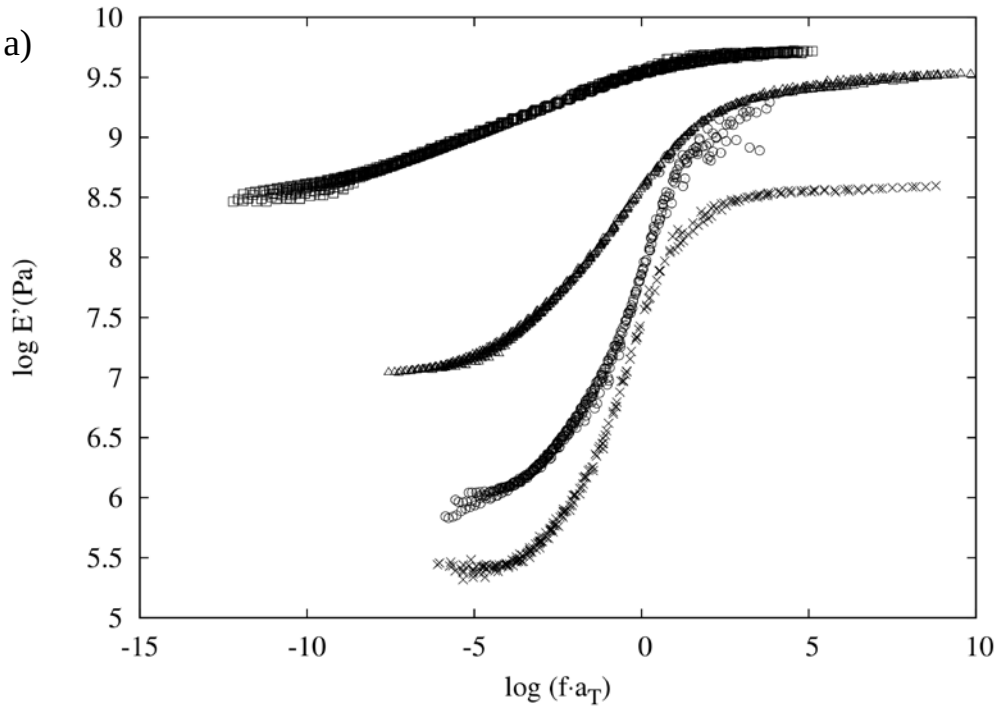

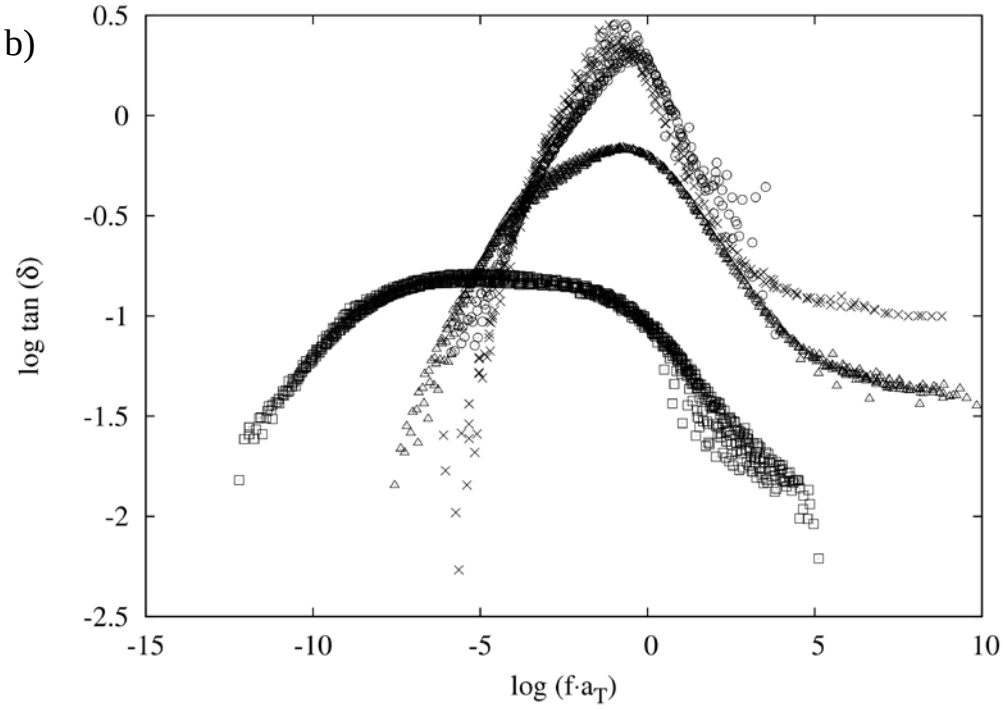

Figure 3. **(a)** Storage modulus (*E'*) and **(b)** loss factor (tan δ) master curves at a reference temperature of 25 ^{0}C for (×) pure PHEA, (⊙) PHEA+10% SiO_2, (△) PHEA+15% SiO_2, (⊡) PHEA+30% SiO_2.

Journal of Macromolecular Science, Part B: Physics, 46:45

From Figure 3a, it can be seen that the storage modulus increases significantly with silica content, both in the glass and in the rubber-like states. The loss factor master curves of pure PHEA and PHEA+10% SiO_2 nearly overlap (Figure 3b). For PHEA-based nanocomposites with 15 and 30 wt% silica, a new relaxation process at lower frequencies (longer times) than the main relaxation peak of the pure PHEA can be detected. For PHEA+15% SiO_2 it appears as a shoulder in the low-frequency side of the main relaxation and it occurs at lower frequencies for the nanocomposite containing 30 wt% silica. The height of the peak appearing at the same frequency as in pure PHEA

decreases with increasing content of silica in the nanocomposite, wheras that of the low-frequency peak increases.

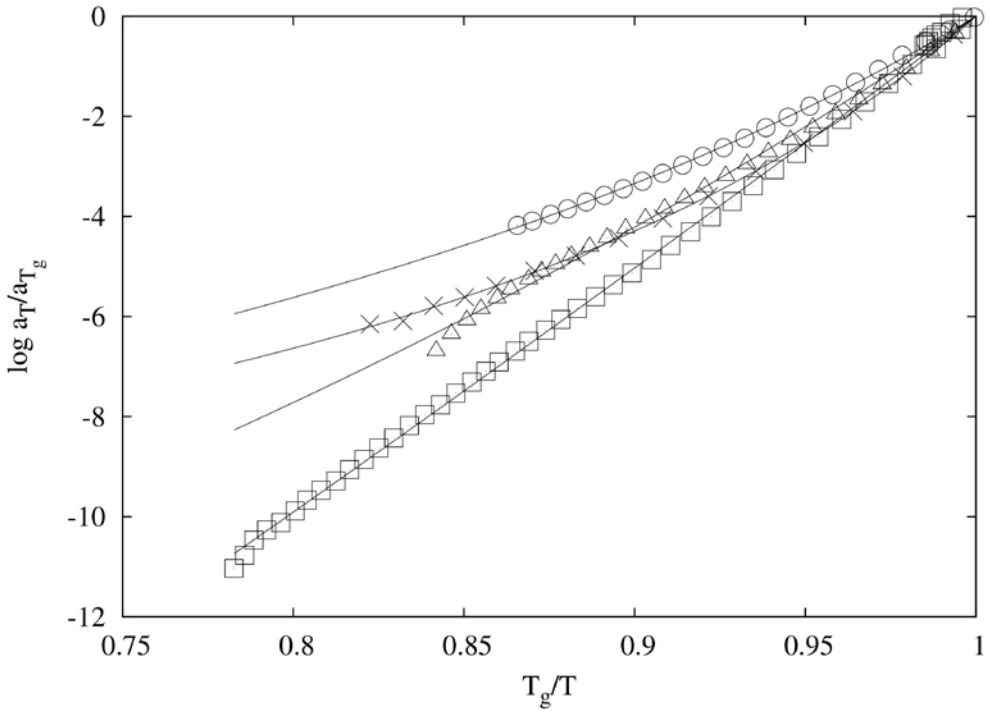

Figure 4. Angell plot of DMS shift factors for (×) pure PHEA, (⊙) PHEA+10% SiO_2, (△) PHEA+15% SiO_2, (⊡) PHEA+30% SiO_2 and the corresponding WLF fit (solid line). The shift factors a_T shown in this figure have been calculated for a reference temperature $T_{ref} = T_g$, where T_g is the glass transition temperature shown in Table 2 calculated from DSC data.

Journal of Macromolecular Science, Part B

The shift factors above T_g, obtained from the construction process of the DMS master curves, were successfully described by the WLF equation (13) – Figure 4:

$$\log a_T = \log \frac{\tau(T)}{\tau(T_{ref})} = -\frac{C_1(T - T_{ref})}{C_2 + (T - T_{ref})} \quad (1)$$

where $\tau(T)$ is the relaxation time at temperature T, and C_1 and C_2 depend on the material and on the reference temperature T_{ref}. This expression usually holds for polymers over the temperature range $T_g<T<T_g+100$ K (where T_g is the glass transition temperature); when T_{ref} is identified with T_g, C_1 and C_2 assume values close to 17.44 and 51.6 K, respectively (13). Equation (1) is in some way equivalent to the Vogel-Fulcher-Tamman-Hesse equation (VFTH) (14-17):

$$\tau(T) = \tau_0 \exp \frac{B}{T - T_0} \quad , T_0<T_g \quad (2)$$

where τ_0 is a pre-exponential factor and B and T_0 are adjustable parameters. The WLF and VFTH equations are the most frequently applied models for describing the non-Arrhenius behaviour of the main relaxation process in glass-forming materials. The WLF and VFTH parameters are related by $C_1 = B/2.303(T_{ref} - T_0)$ and $C_2 = T_{ref} - T_0$ (12); for the studied PHEA nanocomposites they are presented in Table 2.

From the temperature dependence of the shift factor it was possible to calculate the fractional free volume f_g at T_g and the coefficient of volume expansion of the free volume α_f using the relationships (12):

$$f_g = \frac{C_2 + T_g - T_{r_{ef}}}{2.303 C_1 C_2} \quad (3)$$

$$\alpha_f = \frac{1}{2.303 C_1 C_2} \quad (4)$$

Journal of Macromolecular Science, Part B: Physics, 46:43–54, 2007. DOI: 10.1080/00223400601036751

The values of f_g and α_f obtained from DMS results are presented in Figure 5 and Table 2, respectively. A decrease in both parameters (f_g and α_f) is observed as the silica content increases.

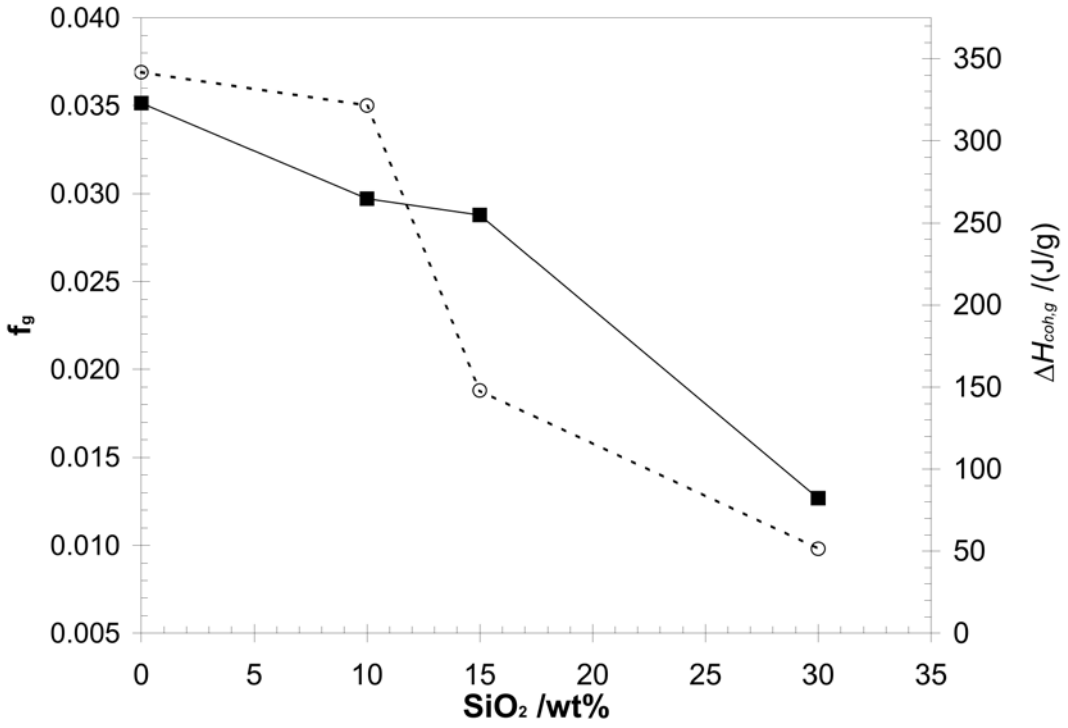

Figure 5. Silica content dependence of the fractional free volume f_g (⊙) and the increment of the specific (polymer mass basis) cohesive energy at T_g, ΔH_g (■).

Journal of Macromolecular Science, Part

3.4. Fragility

Cooperativity plots, or Angell plots, have been used extensively for the analysis of segmental relaxation data (18-20). They represent the rate at which the structural relaxation characteristic time, τ (or related properties, such as the shear viscosity η) decreases with increasing temperature above T_g in a normalised T_g/T plot. From the shift factors of the isothermal results, it was possible to construct the Angell plot for the

samples studied (Figure 4). In this plot, the value of T_g obtained from the DSC data was used.

Fragility is a measure of the magnitude of the decrease of log τ (or log a_T) with decreasing T_g/T and may be characterised by the fragility "index" m:

$$m = \left.\frac{d\log\tau}{d(T_g/T)}\right|_{T=T_g} = \left.\frac{d\log a_T}{d(T_g/T)}\right|_{T=T_g} \quad (5)$$

An m value equal to 16 corresponds to an Arrhenius behaviour ("strong" limit) and for m larger than 200 the systems reaches the "fragile" limit (21). Using Eqs. (1), (2) and (5), m may be directly obtained from the VFTH or WLF parameters:

$$m = \frac{BT_g/2.303}{(T_g - T_0)^2} = \frac{T_g C_1 C_2}{(C_2 + T_g - T_{ref})^2} \quad (6)$$

where C_1 and C_2 are the coefficients of the WLF equation referred to T_{ref}. The values of the fragility index m calculated from Eq. 6 are presented in Table 2, where it is seen that m sharply decreases from pure PHEA to PHEA + 10% SiO_2, and then slowly increases with the silica content.

Journal of Macromolecular Science, Part B: Physics, 46:43–54, 2007. DOI: 10.1080/00223460601036721

3. Discussion

The silica phase obtained under the polymerization conditions of this work exhibits a porous network structure with nanometer-sized pores (22-24) that facilitates its physical interpenetration with the organic polymer chains. The initial H_2O/TEOS ratio was kept constant and equal to 2. Since the amount of acid catalyst was small and the initial H_2O/TEOS ratio is less than 4 (which corresponds to the formation of the stoichiometric fully condensed silica phase (24)), it is expected that an extremely fine network of silica

is formed within the nanocomposite due to polymerising conditions corresponding to slow hydrolysis rate (22). The silica phase presents a bimodal porous distribution, with nanometer-sized pores inside the elementary silica particles on one hand, and the space left between the aggregates of those elementary particles on the other hand (9,20-22); both of them ought to be occupied by PHEA. This structure is seen on the AFM images, where the larger aggregates of the silica phase, in the range of several tens of nanometers, can be identified (Figure 1).

The experimental results suggest that the pure PHEA network and the PHEA domains of the nanocomposites behave differently. On the one hand there is a shift to higher temperatures of the T_g of the PHEA domains in the nanocomposites with respect to the PHEA homopolymer. Although there is not a similar shift in the frequency of the maximum of the loss tangent at 25ºC (Figure 3), the temperature dependence of the shift factors needed to build the master curve shows a behaviour quite different in the bulk PHEA network and in the series of nanocomposites. The fragility is much lower in the nanocomposites than in bulk PHEA. This change of mobility could be due to topological differences in the PHEA network imposed by its polymerization in presence of the silica network.

On the other hand the decrease of Δc_p with increasing silica content implies that there is a fraction of the polymer chains that does not contribute to the glass transition. These immobilized polymer segments could be those within the nanometric pores in the nanoparticles of the silica phase or in the interstices between them, polymer chains that are confined in regions of nanometric dimensions and probably have direct interaction with the silica chains (9).

DMS and DSC results show furthermore that the glass transition temperature and the frequency range in which the main dynamic-mechanical relaxation takes place remain

Journal of Macromolecular Science, Part B: Physics, 46:43–51, 2007 DOI: 10.1080/00222340601036751

almost constant with varying silica content in the nanocomposite, indicating that even in these composites there are enough chains with unrestricted mobility to produce the cooperative motion leading to the main relaxation. However, the decrease of the frequency of the relaxation process of the less mobile chain segments as the silica content increases indicates a change in the number of polymer chains in the above situation and an increasing interaction with the silica network.

It is interesting to remark the change of behaviour shown by the fragility plot with increasing silica content. The shape of the diagram tends to approach an Arrhenius (linear) dependence for the highest silica content and, as a consequence, the difference T_g - T_0 and the value of the parameter B rapidly increase and the fractional free volume and the expansion coefficient of the free volume rapidly decrease with increasing silica content. This means that the segmental dynamics of the PHEA chain segments tends to be less and less cooperative due to the confinement induced by the inorganic phase. This is also reflected in the abnormally high C_1 and C_2 values of the WLF fit of the nanocomposite samples in Table 2, which have the overall effect of decreasing the WLF plot curvature, thus being an additional indication that the behaviour of these samples tends to be more Arrhenius-like. The pattern of the dependence of f_g with the silica content shows a pronounced fall at about 10% silica, probably related to the percolation threshold of the silica network in the nanocomposite. Related to the fragility is the density of cohesive energy of the polymer. This quantity is also an indication of the segmental mobility of the chains (25). An approximate estimate of the change of the cohesive energy density of the polymer at the glass transition, $\Delta H_{coh,g}$, can be obtained from the relationship

$$\Delta H_{coh,g} = C_2 \Delta c_p T_g \,, \qquad (7)$$

Journal of Macromolecular Science, Part B: Physics, 46:43–57, 2007, DOI: 10.1080/00222340601036751

with C_2 = 2.80 ± 10% (25). With the experimental values of Δc_p and T_g given in Table 2 the results represented in Figure 5 are obtained. They show a steady decrease of $\Delta H_{coh,g}$ as the silica content increases. That is: the states of the polymer above and below the glass transition as regards the mobility of its chains are more similar with increasing silica content, consistent with the tendency of the fragility plots to approximate the linear Arrhenius behaviour with increasing silica content of the nanocomposites.

4. Conclusions

Segmental mobility in the PHEA phase of hybrid nanocomposites was studied by dynamic-mechanical analysis and DSC. The mechanical relaxation shows a bimodal relaxation process in the nanocomposites. Physical interactions between the silica and the PHEA chains and the confinement of latter within the silica phase produce a phase of polymer chains with restricted mobility that gives rise to a low-frequency relaxation mechanism whose frequency depends on the silica content. Calorimetric scans are not conclusive as regards the occurrence of a corresponding double glass transition. A broadening of the glass transition and a decrease of the heat capacity increment as silica content increases are manifest, indicating more heterogeneous samples and the constraint of the PHEA matrix leading to a number of immobilized polymer chains that do not contribute to the glass transition.

Journal of Macromolecular Science, Part B: Physics, 46:43–54, 2007, DOI: 10.1080/00223460601036751

Acknowledgements This work was supported by the Spanish Science and Technology Ministry through the project CICyT MAT2002-04239-C03-03. MMP and JLGR want to hommage the unforgettable personality of Valery Pavlovich Privalko, his extraordinary human quality and his fine sense of humour.

References

1. Monleón Pradas, M.; Gómez Ribelles, J.L.; Serrano Aroca, A.; Gallego Ferrer, G.; Suay Antón, J.; Pissis P. Interaction between water and polymer chains in poly(hydroxyethyl acrylate) hydrogels. Colloid Polym. Sci. **2001**, *279*, 323.

2. Dimitriu, S. *Polymeric Biomaterials*; Marcel Dekker: New Cork, 1994.

3. Enderle, J. ; Blanchard, S.; Bronzino, J. *Introduction to biomedical engineering*. Academic Press: San Diego (USA), 2000.

4. Costa, R.; Lameiras, F.S. Structural control in poly(butyl acrylate)-silica hybrids by modifying polymer-silica interactions. J. Sol-Gel Sci. Technol. **2003**, *27*, 343.

5. Li, C.; Wu, J.; Zhao, J.; Zhao, D.; Fan, Q. Effect of inorganic phase on polymeric relaxation dynamics in PMMA/silica hybrids studied by dielectric analysis. Eur. Polym. J. **2004**, *40*, 1807.

6. Huang, S.L.; Chin, W.K.; Yang, W.P. Structural characteristics and properties of silica/poly(2-hydroxyethyl methacrylate) (PHEMA) nanocomposites prepared by mixing colloidal silica or tetraethyloxysilane (TEOS) with PHEMA. Polymer **2005**, *46*, 1865.

7. Matejka, L.; Dusek, K.; Plestil, J.; Kriz, J.; Lednicky, F. Formation and structure of the epoxy-silica hybrids. Polymer **1998,** *40*, 171.

Journal of Macromolecular Science, Part B: Physics, 46:43–54, 2007. DOI: 10.1080/00222340601036751

8. Li, Z.; Hang, W.; Kozodaev, D.; Brokken-Zijp, J.C.M.; de With, G.; Thüne, P.C. Surface properties of poly(dimethylsiloxane)-based inorganic/organic hybrid materials. Polymer **2006**, *47*, 1150.

9. Hajji, P.; David, L.; Gerard, J.F.; Pascault, P.; Vigier, G. Synthesis, structure, and morphology of polymer-silica hybrid nanocomposites based on hydroxyethyl metacrylate. J. Polym Sci. **1999**, *37*, 3172.

10. Grassie, N. Speakman, J.G. Thermal degradation of poly(alkyl acrylates) . I. Preliminary Investigations. J. Polym. Sci., Part A-1, **1971**, *9*, 919.

11. Grassie, N. Speakman, J.G. Davis, T.I. Thermal degradation of poly(alkyl acrylates). II. Primary esters: ethyl, n-propyl, n-butyl, and 2-ethylhexyl. J. Polym. Sci., Part A-1, **1971**, *9*, 931.

12. Ferry, J.D. *Viscoelastic Properties of Polymer*; John Wiley & Sons: New York, 1980.

13. Williams, M.L.; Landel, R.F.; Ferry, J.D. The temperature dependence of relaxation mechanisms in amorphous polymers and other class forming liquids. J. Am. Ceram. Soc. **1955**, *77*, 3701.

14. Williams, G.; Watts D.C.; Dev S.B.; North A.M. Further considerations of non symmetrical dielectric relaxation behaviour arising from a simple empirical decay function. Trans. Faraday Soc. **1971**, *67*, 1323.

15. Vogel H. Das temperatur-abhängigkeitsgesetz der viskosität von lüssigkeiten. Phys. Zeit. **1921**; *22*, 645.

16. Fulcher G.S. Analysis of recent measurements of the viscosity of glasses. J. Am. Ceram. Soc. **1925**, *8*, 339.

Journal of Macromolecular Science, Part B: Physics, 46:43–54, 2007. DOI: 10.1080/00222340601036751

17. Tamman G.; Hesse W. Die Abhängigkeit der Viscosität von der Temperatur bie unterkühlten Flüssigkeiten. Z. Anorg. Allg. Chem. **1926**, *156*, 245.

18. Ediger, M.D.; Angell, C.A.; Nagel, S.R. Supercooled liquids and glasses. J. Phys. Chem. **1996**, *100*, 13200.

19. Plazek, D.J.; Ngai, K.L. Correlation of polymer segmental chain dynamics with temperature-dependent time-scale shifts. Macromolecules **1991**, *24*,1222.

20. Roland, C.M.; Ngai, K.L. Normalization of the temperature dependence of segmental relaxation times. Macromolecules **1992**, *25*, 5765.

21. Böhmer, R.; Ngai, K.L.; Angell, C.A.; Plazek, D.J. Nonexponential relaxations in strong and fragile glass formers. J. Chem. Phys. **1993**, *99*, 4201.

22. Brinker, C.J.; Keefer, K.D.; Schaefer, D.W.; Ashley, C.S. Sol-gel transition in simple silicates. J. Non-Cryst. Solids **1982**, *48*, 47.

23. Rubio, F.; Rubio, J.; Oteo, J.L. Further insights into the porous structure of TEOS derived silica gels. J. Sol-Gel Sci. Technol.**1997**, *8*: 159.

24. Strawbridge, I.; Craievich, A.F.; James, P.F. The effect of the H_2O/TEOS ratio on the structure of gels derived by the acid catalysed hydrolysis of tetraethoxysilane. J. Non-Cryst. Solids **1985,** *72*,139.

25. В. П. Привалко. *Молекулярное Строение и Свойства Полимеров*. Химия, Ленинград, 1986 (V. P. Privalko. *Molecular Structure and Properties of Polymers (in russian)*. Khimiya, Leningrad, 1986). Page 85.

Journal of Macromolecular Science, Part B: Physics, 46:3–54, 2007. DOI: 10.1080/00222340601036751